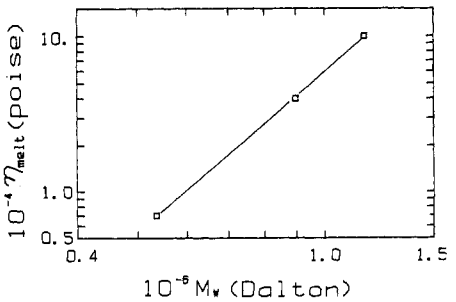

Figure 10. log–log plot of η_{melt} vs. M_w at 297 °C. $\eta_{melt} = 1.88 \times 10^{-20} M_w^{3.42}$, with η_{melt} and M_w expressed in units of poise and daltons, respectively.

confirming the experimental viscosity exponent of 3.4. With eq 7, it is now possible to determine the molecular weight of PETFE in the melt state by means of high-temperature rheometry so long as the molecular weight of PETFE remains sufficiently high for the melt viscosity exponent value of 3.4 to hold.

IV. Conclusions

Laser light scattering, including measurements of the angular distribution of the absolute scattered intensity and of the time correlation function together with correlation function profile analysis, has been developed into a powerful analytical tool for polymer characterizations. We have succeeded in determining the molecular weight and its distribution of polymers, which are very difficult to characterize by standard analytical techniques. Aside from polyethylene in trichlorobenzene, poly(1,4-phenyleneterephthalamide) in concentrated sulfuric acid, and poly(ethylene terephthalate) in hexafluoro-2-propanol, we have now characterized an alternating copolymer of ethylene and tetrafluoroethylene. In each case, the problem has often been much more than just searching for an appropriate solvent for the polymer. For the PETFE characterization, we had to develop a new apparatus for polymer dissolution and solution clarification at high temperatures, a new light scattering spectrometer, and improved methods of data analysis. The technology has now been developed and demonstrated under the most stringent conditions. By coupling with other separation techniques, the LLS detection technique using a flow cell[14] should have great potential as an analytical tool for polymer and colloidal particle characterizations.

Acknowledgment. We gratefully acknowledge support of this research by the National Science Foundation, Polymers Program (Grant DMR 8314193), the Petroleum Research Fund, administered by the American Chemical Society, and the U.S. Army Research Office (Contracts DAAG2985K0067 and DAAG2984G0080).

Registry No. (TFE)(E) (copolymer), 25038-71-5.

References and Notes

(1) See: Schulz-DuBois, E. O., Ed. *Proceedings of the 5th International Conference on Photon Correlation Techniques in Fluid Mechanics* (Springer Series in Optical Sciences); Springer-Verlag: New York, 1983.
(2) Chu, B.; Ford, J. R.; Dhadwal, H. S. In *Methods Enzymol.* **1983**, *117*, 256–297.
(3) Pope, J. W.; Chu, B. *Macromolecules* **1984**, *17*, 2633.
(4) McWhirter, J. G.; Pike, E. R. *J. Phys. A* **1978**, *11*, 1729.
(5) Ostrowski, N.; Sornette, D.; Parker, P.; Pike, E. R. *Opt. Acta* **1981**, *28*, 1059.
(6) Chu, B.; Ying, Q.-C.; Wu, C.; Ford, J. R.; Dhadwal, H. S. *Polymer* **1985**, *26*, 1408.
(7) Provencher, S. W. *Biophys. J.* **1976**, *16*, 27; *J. Chem. Phys.* **1976**, *64*, 2772; *Makromol. Chem.* **1979**, *180*, 201.
(8) Koppel, D. E. *J. Chem. Phys.* **1972**, *57*, 4814.
(9) Abbiss, J. B.; Demol, C.; Dhadwal, H. D. *Opt. Acta* **1983**, *30*, 107.
(10) Chu, B. In *The Application of Laser Light Scattering to the Study of Biological Motion*; Earnshaw, J. C., Steer, M. W., Eds.; Plenum: New York, 1983; pp 53–76.
(11) See for example: Miller, K. *SIAM J. Math. Anal.* **1970**, *1*, 52. Tikhonov, A. N.; Arsenin, V. Y. *Solutions of Ill-Posed Problems*, V. H. Winston: Washington, D.C., 1977.
(12) Chu, B. *Polym. J. (Tokyo)* **1985**, *17*, 225.
(13) Chu, B.; Wu, C.; Ford, J. R. *J. Colloid Interface Sci.* **1985**, *105*, 473.
(14) Chu, B.; Park, I. H.; Ford, J. R. *Polym. Prepr. (Am. Chem. Soc., Div. Polym. Chem.)* **1983**, *24*, 237.
(15) English, A. D.; Garza, O. T. *Macromolecules* **1979**, *12*, 351.

Dynamics of a Flexible Polymer Chain in Steady Shear Flow: The Rouse Model

J. A. Y. Johnson*

Hasbrouck Laboratory, Department of Physics and Astronomy, University of Massachusetts, Amherst, Massachusetts 01003. *Received June 9, 1986*

ABSTRACT: The Rouse model of a flexible polymer in dilute solution is studied. A complete description of the dynamics of a Hookean dumbbell in shear flow is developed from the Bose operator representation of the Smoluchowski equation. The relaxation of fluctuations from the nonequilibrium steady state is examined, and dynamic correlation functions are determined exactly. The results are used to study the dynamics of the Rouse chain in shear flow.

I. Introduction

The theoretical study of dilute polymer solutions has contributed considerably to the understanding of polymer flow properties (see, e.g., ref 1–4). In dilute solutions, with which this paper is concerned, interchain interactions are negligible, and, therefore, each chain contributes independently to the flow properties and can be treated separately. The bead–spring models, which represent a polymer molecule by a chain of beads connected by springs (see Figure 1), have had notable success in describing dilute solutions of flexible polymers.[2] In these models, the springs represent nearest-neighbor interactions between beads, which represent segments of the polymer; non-nearest-neighbor interactions can also be included. The beads also

* Present address: Department of Polymer Science and Engineering, University of Massachusetts, Amherst, MA 01003.

0024-9297/87/2220-0103$01.50/0

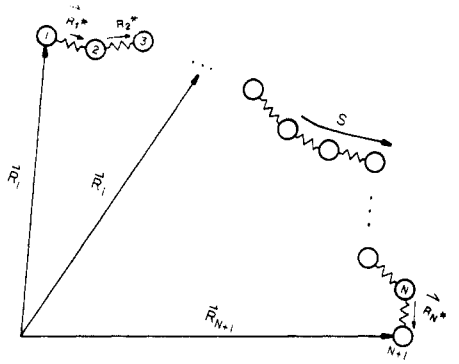

Figure 1. Bead–spring model. A bead–spring model of a polymer consists of $N + 1$ beads connected by N springs. The vector $\vec{R}_i$ indicates the position of the ith bead. $\vec{R}_i^*$ is the dimensionless relative coordinate: $l\vec{R}_i^* = \vec{R}_{i+1} - \vec{R}_i$.

interact with the solvent molecules, that is, the fluid in which they are embedded. Usually this interaction is approximated by a frictional force, which is proportional to the relative velocity between the bead and the solvent, and by a random stochastic force.[2] Thus, the beads are treated as interacting, classical, Brownian particles. This leads to a description of the chain in terms of a probability distribution function for the positions and velocities of the beads, whose time evolution is given by the Fokker–Planck equation.[5] If the time scale over which the velocities of the beads approach their equilibrium values is much shorter than that over which the positions of the beads approach their equilibrium values, then the Fokker–Planck equation reduces to a generalized diffusion, or Smoluchowski, equation.[6] This is referred to as the strong-damping limit and is appropriate for polymer solutions. The Smoluchowski equation (SE) describes the time evolution of the probability distribution function of the chain in configuration space. The SE description has been used to study polymer solutions under various conditions. The most prevalent use by far has been in studies of equilibrium statistical mechanics and dynamics; that is, the focus has been on describing the average equilibrium configuration of a chain in a solvent at rest (or in uniform motion) and the time dependence of fluctuations out of that configuration. It has been used less frequently to study nonequilibrium behavior, such as the behavior of a polymer in a solvent undergoing flow. In nonequilibrium studies, the emphasis has been on steady-state statistical mechanics, i.e., on determining the time-independent properties of chains in a steady, time-independent, flow field. Examples of this application of the SE description are given in ref 7. Much less attention has been given to nonequilibrium steady-state (NESS) statistical dynamics, i.e., the description of the time-dependent fluctuations around the NESS.[8] This is the application to which the present work is addressed. (Dotson[9] has treated nonequilibrium dynamics using molecular dynamics simulations based on the Langevin equation. His results should be comparable to the results obtained here.) A last application of the SE approach is to describe the average, time-dependent, behavior of a chain in a time-dependent flow field. See, for examples, ref 10.

We consider a polymer chain in a solvent undergoing steady shear flow, the simplest nonpotential flow, for which the velocity field is $\vec{v} = y\hat{x}$. Potential flow is that for which the velocity field can be written as the gradient of a potential. A system undergoing potential flow is formally equivalent to a system in equilibrium, since the presence of the flow has the same effect on the polymer chain as an external potential (albeit, usually, an anisotropic one).[2]

We will employ the Rouse model of a flexible polymer chain, which is in the fundamental bead–spring model (and call the polymer chain a Rouse chain).[11] The time-independent distribution function for a Rouse chain (i.e., the steady-state distribution function) in shear flow is well-known.[1,2] We investigate the time-dependent behavior. We will not, however, in this first study, include hydrodynamic interactions or excluded volume effects, since including them would have to be done self-consistently. That is, we would need to consider the effect of the shear flow on both the hydrodynamic interactions, as in ref 12, and the excluded volume interactions. Furthermore, since we are treating dynamics, the frequency dependence of the hydrodynamic interactions might also need to be included. (These self-consistency requirements have been noted previously by Fixman[13] and by Edwards and Freed.[14]) Thus, we ignore both effects in this initial investigation in order to clarify the important behavior that arises from the shear flow itself.

In the next section, we discuss the SE for the Rouse chain in detail. In section III, we specialize to the case of a Hookean dumbbell and introduce the Bose operator formalism with which we derive our results. We use the dumbbell results from section III for the Rouse chain in section IV. Section V contains a summary of our results and some concluding remarks. Some mathematical details are given in the appendices.

II. Smoluchowski Equation

In bead–spring models of a polymer in dilute solutions, each bead has an equation of motion determined by the bead–bead, bead–solvent, and external forces. Introducing a friction coefficient and a stochastic force to approximate the bead–solvent interaction, as discussed in the Introduction, leads to the Langevin equation of motion for the ith bead:

$$m\dot{\vec{v}}_i + \zeta(\vec{v}_i - \vec{u}_i) = \vec{f}_i + \vec{F}_i \qquad \text{(II.1)}$$

Here, m is the mass of the ith bead, $\vec{v}_i$ is its velocity, ζ is the friction coefficient, and $\vec{u}_i$ is the velocity of the solvent at the position of the ith bead, $\vec{u}(\vec{R}_i)$. We take ζ and m to be the same for all beads. $\vec{f}_i$ and $\vec{F}_i$ are the stochastic and deterministic forces, respectively. The second term on the left-hand side, due to friction between bead and solvent, works to drive the velocity of a particle at $\vec{R}$ to $\vec{u}(\vec{R})$, the flow velocity of the solvent at $\vec{R}$. The flow field of the solvent is imposed on it from outside and is not changed by the presence of the polymers.

It is desirable to employ a statistical description of the polymer solution because of the stochastic forces in eq II.1. The Fokker–Planck equation for the distribution function of the polymer can be derived from the Langevin equation[5] and can then be expanded for large friction.[6] Assuming the following statistical properties for the stochastic forces

$$\begin{aligned} \langle \vec{f}_i(t) \rangle &= 0 \\ \langle \vec{f}_i(t)\vec{v}_j(t') \rangle &= 0 \\ \langle \vec{f}_i(t)\vec{f}_j(t') \rangle &= 2kT\zeta\delta_{ij}\delta(t-t') \end{aligned} \qquad \text{(II.2)}$$

leads to the usual SE for the probability distribution function Φ for the entire chain:[15]

$$[\partial_t + \vec{u}\cdot\vec{\nabla}]\Phi(\vec{\mathcal{R}}t) = D\vec{\nabla}\cdot[\vec{\nabla} + (\vec{\nabla}\beta V)]\Phi(\vec{\mathcal{R}}t) \qquad \text{(II.3)}$$

The right-hand side of this equation is the generalized diffusion operator, in which the first term is the usual diffusion operator and the second term accounts for any nonstochastic forces. $\vec{\mathcal{R}}$ is a $3(N + 1)$-dimensional vector representing the three spatial coordinates of the $N + 1$

beads. Thus, the scalar products are $3(N+1)$-dimensional dot products. The diffusion coefficient is related to ζ by the Einstein relation $D = kT/\zeta$, and $\beta \equiv 1/kT$. V is the spring potential. (The Rouse model employs a Hookean potential with spring constant Γ, $V = {}^1/_2\Gamma\sum(\vec{R}_{i+1}-\vec{R}_i)^2$; other choices of V define other bead–spring models.) The left-hand side is the total time derivative of the distribution function. It has been assumed that the solvent is incompressible and that the flow field has neither sources nor sinks; that is, $\vec{\nabla}\cdot\vec{u} = 0$. This condition is satisfied by shear flow, for which $\vec{u}_i = \dot{\gamma}\Lambda\cdot\vec{R}_i$, where $\dot{\gamma}$ is the shear rate and $\Lambda_{ij} = \delta_{1i}\delta_{2j}$. Once $\Phi(\vec{\mathcal{R}},t)$ is known, it can be used to calculate averages and correlation functions. The average of a function $A(\vec{\mathcal{R}})$ at time t is given by

$$\langle A(t)\rangle = \int d\vec{\mathcal{R}}\, A(\vec{\mathcal{R}})\Phi(\vec{\mathcal{R}},t) \qquad \text{(II.4)}$$

The correlation between a function $A(\vec{\mathcal{R}})$ at time t and $B(\vec{\mathcal{R}})$ at time t_0 is given by

$$\langle A(t)B(t_0)\rangle = \int d\vec{\mathcal{R}}'\, d\vec{\mathcal{R}}\, A(\vec{\mathcal{R}})\Phi(\vec{\mathcal{R}},t|\vec{\mathcal{R}}',t_0)B(\vec{\mathcal{R}}')\Phi(\vec{\mathcal{R}}',t_0) \qquad \text{(II.5)}$$

where $\Phi(\vec{\mathcal{R}},t|\vec{\mathcal{R}}',t_0)$ is the conditional probability that the configuration of the polymer is $\vec{\mathcal{R}}$ at time t given that the configuration was $\vec{\mathcal{R}}'$ at time t_0.

We will write the SE and the potential in terms of dimensionless coordinates. To this end, we define a characteristic length l and a characteristic time τ by

$$l^2 = (\beta\Gamma)^{-1}$$

and

$$\tau = \zeta/\Gamma \qquad \text{(II.6a)}$$

with which we define the following dimensionless quantities:

$$\text{(a) } \vec{\mathcal{R}} = \vec{\mathcal{R}}/l$$
$$\text{(b) } \vec{u}_0 = \vec{u}/\dot{\gamma}l$$
$$\text{(c) } \sigma = \dot{\gamma}\tau$$
$$\text{(d) } t = t/\tau \qquad \text{(II.6b)}$$

(In a bead–spring model other than the Rouse model, Γl^2 can be replaced by some appropriate energy scale.) In terms of these parameters, the SE is

$$[\partial_t + \sigma\vec{u}_0\cdot\vec{\nabla}]\Phi(\vec{\mathcal{R}}) = \vec{\nabla}\cdot[\vec{\nabla} + (\vec{\nabla}\beta V)]\Phi(\vec{\mathcal{R}}) \qquad \text{(II.7)}$$

A. Equilibrium. General Bead–Spring Models. For a chain in equilibrium, the behavior of the function Φ is understood thoroughly for the Rouse model. For other models, however, only some general properties have been deduced. We will derive these general properties here and will then specialize to the Rouse model. This exercise will serve several purposes: First, we will be able to compare equilibrium to the NESS and thereby illustrate the additional mathematical difficulties that are encountered in the study of shear flow. Second, we will derive some results for the Rouse model, in this simpler context, which will be used later. Last, we will be able to compare the properties of the Rouse model in equilibrium, as derived here, with its properties in steady shear, to be derived in sections III and IV.

In equilibrium, for which $\sigma = 0$, the time-independent solution Φ_0 to the SE in eq II.7 is the Boltzmann distribution:

$$\Phi_0 = J_0 \exp(-\beta V) \equiv \Psi_0{}^2 \qquad \text{(II.8)}$$

J_0 is a normalization factor. This equation also defines a new function Ψ_0, which is needed below. To find the time-dependent solutions, which represent equilibrium fluctuations, we define a new function Ψ such that

$$\Phi \equiv \Psi_0\Psi \qquad \text{(II.9)}$$

Using this definition in eq II.7, with $\sigma = 0$, leads to an equation of motion for Ψ.

$$\partial_t\Psi = -[-\nabla^2 + {}^1/_4(\vec{\nabla}\beta V)^2 - {}^1/_2(\nabla^2\beta V)]\Psi \equiv -S\Psi \qquad \text{(II.10)}$$

It is important to note that the operator S defined in eq II.10 is a Hermitian operator. More specifically, it has the same form as the Hamiltonian operator in quantum mechanics. Therefore, we will refer to Ψ in eq II.10 as the "wave function", to distinguish it from Φ, the probability distribution function.

The formal solution to eq II.10 is

$$\Psi(t) = e^{-St}\Psi(0) \qquad \text{(II.11)}$$

where $\Psi(0)$ is the wave function at $t = 0$. The Hermiticity of S ensures that it has a complete set of orthonormal eigenfunctions Ψ_ν and real eigenvalues λ_ν, determined by

$$S\Psi_\nu = \lambda_\nu\Psi_\nu \qquad \text{(II.12)}$$

Thus, $\Psi(0)$ can be expanded in terms of these eigenfunctions:

$$\Psi(0) = \sum_\nu C_\nu\Psi_\nu \qquad \text{(II.13)}$$

Using this expansion in eq II.11 leads to an eigenfunction expansion for $\Psi(t)$:

$$\Psi(t) = \sum_\nu C_\nu e^{-\lambda_\nu t}\Psi_\nu \qquad \text{(II.14)}$$

We use the language of quantum mechanics once more and refer to Ψ_ν as the νth "state". If $C_\nu \neq 0$, then the νth state is occupied; otherwise, it is not occupied.

Note that the ground state ($\nu = 0$) is Ψ_0 and has $\lambda_0 = 0$ (as evidenced by $S\Psi_0 = 0$). Normalization requires that $\int\Phi\, d\vec{\mathcal{R}} = \int\Psi_0\Psi\, d\vec{\mathcal{R}} = 1$. Using the expansion of eq II.14 and the orthonormality of the eigenfunctions, this condition leads to

$$C_0 = 1 \qquad \text{(II.15)}$$

for any t. Equation II.15 is simply a statement of the conservation of probability. Thus, the ground state is always occupied with amplitude 1. If any excited state ($\nu \neq 0$) is initially occupied, then its amplitude decays exponentially in time, with time constant $\lambda_\nu{}^{-1}$. These states correspond to equilibrium fluctuations; that is, fluctuations around the average behavior of the chain in equilibrium. That they decay exponentially follows directly from the Hermiticity of S and is a result that is valid for any bead–spring model in equilibrium (i.e., for any V in eq II.10).

Averages and correlation functions can be expressed in terms of the wave functions. Using eq II.4 and assuming the system is in the ground state (i.e., $\Phi(\vec{\mathcal{R}},t) = \Psi_0{}^2(\vec{\mathcal{R}})$), we find

$$\langle A(t)\rangle = \langle A\rangle = \langle 0|S|0\rangle \qquad \text{(II.16)}$$

The last expression is written in Dirac notation, which is defined by

$$\langle\mu|A|\nu\rangle = \int d\vec{\mathcal{R}}\, \Psi_\mu(\vec{\mathcal{R}})A(\vec{\mathcal{R}})\Psi_\nu(\vec{\mathcal{R}}) \qquad \text{(II.17)}$$

A correlation function in equilibrium can be written in terms of the wave function by using eq II.5 and taking

$$\Phi(\vec{\mathcal{R}}',t_0) = \Psi_0{}^2(\vec{\mathcal{R}}') \qquad \text{(II.18)}$$

and

$$\Phi(\vec{\mathcal{R}}t|\vec{\mathcal{R}}'t_0) = \Psi_0(\vec{\mathcal{R}},t)e^{-(t-t_0)S(\vec{\mathcal{R}})}\left[\frac{\delta(\vec{\mathcal{R}}-\vec{\mathcal{R}}')}{\Psi_0(\vec{\mathcal{R}}'t_0)}\right] \quad \text{(II.19)}$$

This leads to

$$\langle A(t)B(t_0)\rangle = \langle 0|Ae^{-S(t-t_0)}B|0\rangle = \sum e^{-\lambda_\nu(t-t_0)}\langle 0|A|\nu\rangle\langle\nu|B|0\rangle \quad \text{(II.20)}$$

Note that the exponential decay of the wave functions leads to an exponential decay of correlation functions.

Rouse Model. Having considered the general properties of bead–spring models, we now turn our attention to the Rouse model, for which the potential V is

$$\beta V = \tfrac{1}{2}\sum_1^N(\vec{R}_{i+1} - \vec{R}_i)^2 \quad \text{(II.21)}$$

This form suggests that we transform to the coordinates defined by

$$\vec{R}_i^* = \vec{R}_{i+1} - \vec{R}_i; \qquad i = 1, ..., N$$

$$\vec{R}^*_{N+1} = \vec{R}_c^* = \frac{1}{N}\sum\vec{R}_j \quad \text{(II.22)}$$

This transformation to relative and center of mass coordinates can be summarized by the matrix equation[2]

$$\vec{\mathcal{R}}^* = \mathbf{B}\cdot\vec{\mathcal{R}}$$

where

$$B_{ij} = \delta_{i+1,j} - \delta_{i,j}; \qquad i = 1, ..., N$$

$$B_{ij} = 1/(N+1); \qquad i = N+1, \text{ for all } j$$

$\vec{\mathcal{R}}^*$ is a $3(N+1)$-dimensional vector whose first $3N$ components are the relative coordinates between the beads and whose last 3 components are the center of mass coordinates $\vec{R}_c^*$. In terms of these coordinates, the potential is

$$\beta V = \tfrac{1}{2}\sum\vec{R}_i^{*2} = \tfrac{1}{2}\vec{\mathcal{R}}^*\cdot\vec{\mathcal{R}}^* \quad \text{(II.23)}$$

and the SE in equilibrium is

$$\partial_t\Phi(\vec{\mathcal{R}}^*) = \vec{\nabla}\cdot\mathbf{A}\cdot[\vec{\nabla} + (\vec{\nabla}\beta V)]\Phi(\vec{\mathcal{R}}^*) \quad \text{(II.24)}$$

where $\mathbf{A}$ is the $N \times N$ Rouse matrix. It is defined by

$$A_{ij} = 2\delta_{ij} - \delta_{i,j\pm1} \quad \text{(II.25)}$$

The dot products are now $3N$ dimensional. The center of mass dependence of the distribution function has been separated out. On average, the center of mass of the chain moves with the local solvent velocity. It can be taken as the origin of the coordinate system and need not be considered further. The behavior of the center of mass coordinate is addressed in detail in ref 2, as is the transformation to normal coordinates, which is summarized below.

Any further progress requires that we transform to normal coordinates—those coordinates in which the Rouse matrix $\mathbf{A}$ is diagonal. This is accomplished through the use of the unitary transformation $\mathbf{U}$ defined by

$$U_{kj} = \left(\frac{2}{N+1}\right)^{1/2}\sin\left(\frac{kj\pi}{N+1}\right) \quad \text{(II.26)}$$

$\mathbf{U}$ has the following properties:

$$\mathbf{U}^\dagger\mathbf{U} = \mathbf{I}$$

$$(\mathbf{U}^\dagger\mathbf{A}\mathbf{U})_{jk} = a_j\delta_{jk} \quad \text{(II.27)}$$

where a_j is the jth eigenvalue of $\mathbf{A}$ and is given by

$$a_j = 4\sin^2\left(\frac{j\pi}{2(N+1)}\right) \quad \text{(II.28)}$$

The normal coordinates $\vec{\mathcal{Q}}$ and the potential V are given by

$$\vec{\mathcal{Q}} = \mathbf{U}^\dagger\cdot\vec{\mathcal{R}}^*$$

$$\beta V = \tfrac{1}{2}\sum\vec{Q}_i^2 = \tfrac{1}{2}\vec{\mathcal{Q}}\cdot\vec{\mathcal{Q}} \quad \text{(II.29)}$$

Again, the script notation $\vec{\mathcal{Q}}$ refers to a $3N$-dimensional vector whose N three-dimensional components are denoted by $\vec{Q}_i$ ($i = 1, ..., N$). In terms of the normal coordinates, the equilibrium SE, eq II.24, becomes

$$\partial_t\Phi(\vec{\mathcal{Q}}) = \sum a_\alpha\vec{\nabla}_\alpha\cdot[\vec{\nabla}_\alpha + (\vec{\nabla}_\alpha\beta V)]\Phi(\vec{\mathcal{Q}}) \quad \text{(II.30)}$$

The equation for the wave function Ψ, eq II.10, is

$$\partial_t\Psi = \sum a_\alpha[\vec{\nabla}_\alpha\cdot\vec{\nabla}_\alpha - \tfrac{1}{4}(\vec{\nabla}_\alpha\beta V\cdot\vec{\nabla}_\alpha\beta V) + \tfrac{1}{2}(\vec{\nabla}_\alpha\cdot\vec{\nabla}_\alpha\beta V)]\Psi \equiv -\sum a_\alpha S_\alpha\Psi \quad \text{(II.31)}$$

Equations II.30 and II.31 are separable in this form, provided $\vec{\nabla}_\alpha\beta V$ is a function of $\vec{Q}_\alpha$ only, as in the Rouse model. Therefore, we use a product wave function defined by

$$\Psi = \prod_\alpha\psi_\alpha; \qquad \alpha = 1, ..., N \quad \text{(II.32)}$$

where $\psi_\alpha \equiv \psi_\alpha(\vec{Q}_\alpha)$. Equation II.31 becomes a set of N equations

$$\partial_t\psi_\alpha = -a_\alpha S_\alpha\psi_\alpha \quad \text{(II.33)}$$

The explicit form of S_α for the Rouse model is

$$S_\alpha = -\vec{\nabla}_\alpha^2 + \tfrac{1}{4}\vec{Q}_\alpha^2 - \tfrac{3}{2} \quad \text{(II.34)}$$

Equation II.32 can be further separated spatially. That is, we can write ψ_α as a product wave function

$$\psi_\alpha = \psi_\alpha^x\psi_\alpha^y\psi_\alpha^z \quad \text{(II.35)}$$

where ψ_α^i is a function only of the ith spatial component of $\vec{Q}_\alpha$. Thus, eq II.33 can be written as a set of three equations

$$\partial_t\psi_\alpha^i = -a_\alpha S_\alpha^i\psi_\alpha^i; \qquad i = 1, 2, 3 \quad \text{(II.36)}$$

where

$$S_\alpha^i = -(\partial_\alpha^i)^2 + \tfrac{1}{4}(Q_\alpha^i)^2 - \tfrac{1}{2} \quad \text{(II.37)}$$

The eigenstates of S_α^i are those of the one-dimensional quantum harmonic oscillator. Thus, the nth eigenstate of S_α is

$$(\psi_\alpha^i)_n = H_n\left(\frac{Q_\alpha^i}{2^{1/2}}\right)\exp[-\tfrac{1}{4}(Q_\alpha^i)^2] \quad \text{(II.38)}$$

(where H_n are the Hermite polynomials) and has eigenvalue $(\lambda_\alpha^i)_n = n$. Eigenstates of the full operator are products of the ψ_α^i and the eigenvalues are sums of the λ_α^i. It is worth emphasizing that (1) each normal mode is decoupled from the other normal modes (that is, ψ_α is not coupled to ψ_β), (2) a given excited state of a specific normal mode is not coupled to other excitations of that normal mode (the nth is not coupled to the mth), and (3) an excitation in a specific spatial direction is not coupled to excitations in another spatial direction (that is, the distribution is spherically symmetric). We make note of this behavior to have it available for comparison with the behavior in shear flow.

B. Steady State. Statics. In a steady shear flow, general solutions to the SE are not known. This is in contrast to equilibrium, for which at least the time-independent distribution function (eq II.8) is known. For the

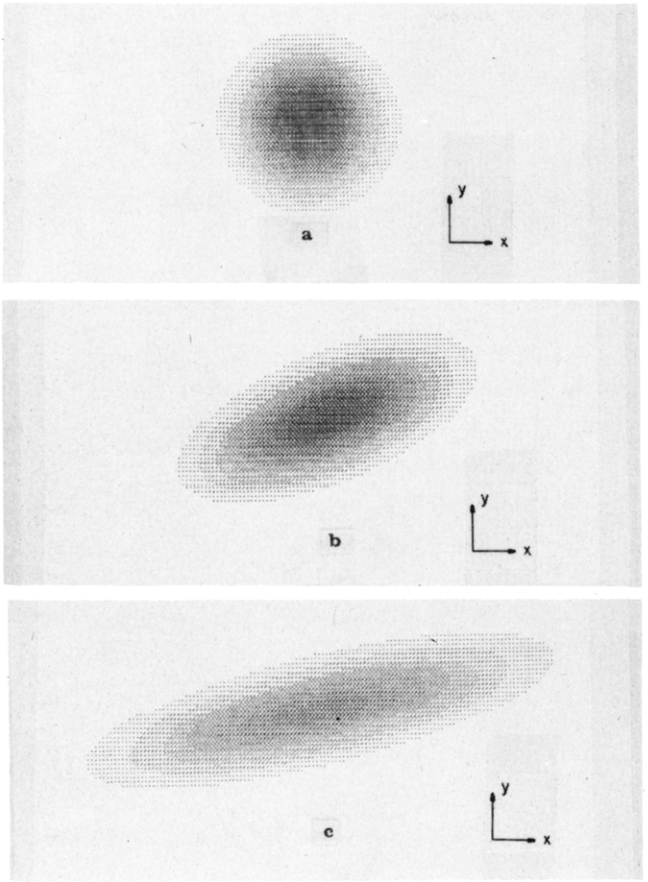

Figure 2. Steady-state distribution function ϕ_0. The steady-state distribution function ϕ_0 given in eq II.42 is plotted as a function of x and y; the z dependence has been integrated out. The density of dots is proportional to $\phi_0(x,y)$. (a) $\xi = 0$. The equilibrium distribution is isotropic. There is no coupling between x and y. (b) $\xi = 1$. When shear flow is present, the distribution function becomes ellipsoidal. The major axis of the ellipsoid makes an angle θ with the x axis, where θ is defined in eq III.1. The distribution function is broader in x than in y, and it is more probable that x and y have the same sign than opposite signs. (c) $\xi = 2$. Stronger flow gradients lead to increased anisotropy and further elongation of the distribution function.

Rouse model in steady shear flow, the time-independent solution to eq II.3 is known and is exhibited below. Writing the dimensionless velocity field at the ith bead as

$$\vec{u}_{0,i} = \Lambda \cdot \vec{R}_i \tag{II.39}$$

where Λ is defined below eq II.3, and

$$\Phi = \prod_\alpha \phi_\alpha \tag{II.40}$$

the SE for the αth normal coordinate is

$$[\partial_t + \sigma(\Lambda \cdot \vec{Q}_\alpha)\cdot\vec{\nabla}_\alpha]\phi_\alpha = a_\alpha \vec{\nabla}_\alpha \cdot [\vec{\nabla}_\alpha + (\vec{\nabla}_\alpha \beta V)]\phi_\alpha \tag{II.41}$$

The form of the time-independent solution for each of the $3N$ modes is (omitting the subscript α)

$$\phi_0 = J_0 \exp\left\{-\tfrac{1}{2}\frac{(x - \xi y)^2}{1 + \xi^2} + y^2 + z^2\right\} \tag{II.42}$$

where x, y, and z refer to the spatial components of Q_α and $\xi_\alpha = \sigma/(2a_\alpha)$. It is evident from eq II.41 that, when $\sigma \neq 0$, the normal modes continue to be independent of one another. The shear flow does, however, effect a coupling between the x and y directions. This is illustrated for a Hookean dumbbell ($N = 1$) in Figure 2. A Hookean dumbbell has only one normal coordinate; it corresponds to the separation vector between the two beads. The eigenvalue is $a = 2$ and therefor $\xi = \sigma/4$. Figure 2 shows plots of the probability density ϕ_0, from eq II.42, as a function of x and y (z has been integrated out) for several values of σ. Clearly, contours of equal probability would be ellipses. As the flow rate σ increases, the coupling between x and y increases, the distribution becomes more elongated, and the symmetry axes rotate further toward the coordinate axes. This is the behavior one would expect physically. When the two beads fluctuate around their average position ($\vec{Q}_\alpha = 0$), they experience differing velocity fields due to the velocity gradient. The resulting difference in the frictional force acting on each is such that there is a force couple acting on the dumbbell which tends to elongate and rotate it. This is illustrated qualitatively in Figure 3.

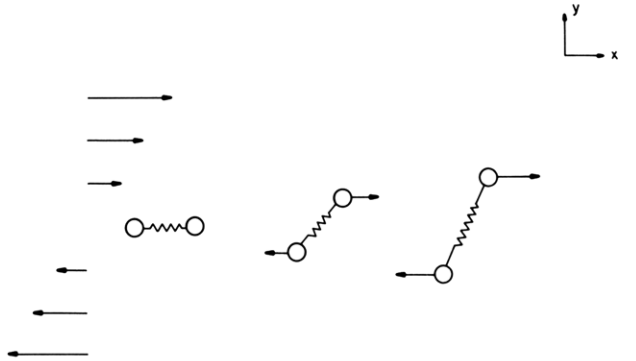

Figure 3. Force couple on a dumbbell in shear flow. The arrows at the left of the figure indicate the velocity of the solvent as seen from the center of mass of the dumbbell. If both beads have the same y coordinate, then there is no difference in the friction force acting on each of them. If the beads are separated in the y direction, then the friction forces acting on them are in opposite directions; consequently, the dumbbell is stretched in the x direction. The stretching is proportional to the separation in the y direction; i.e., $x \sim \xi y$.

For chains of $N + 1$ beads, the strength of the coupling, ξ_α, is different for each mode. For the low-lying modes, a_α is small and ξ_α is very large. For the higher modes, $a_\alpha \to 4$, and the coupling decreases. This can also be understood on physical grounds. The low-lying modes correspond to long-wavelength fluctuations. Hence, they probe long distance scales and experience large differences in the frictional forces. The high-lying modes correspond to short-wavelength fluctuations and therefore probe only short distance scales. Thus, the low-lying modes contribute more significantly to the overall distortion of the chain than do the higher modes. This appears in eq II.42 as a larger coupling constant ξ.

Dynamics. We will now investigate the time-dependent behavior of a Rouse chain in a steady shear flow, as described by eq II.41. If we rewrite eq II.41 as

$$[\partial/\partial t_\alpha + 2\xi_\alpha(\Lambda \cdot \vec{Q}_\alpha)\cdot\vec{\nabla}_\alpha]\phi_\alpha = \vec{\nabla}_\alpha \cdot [\vec{\nabla}_\alpha + (\vec{\nabla}_\alpha \beta V)]\phi_\alpha \tag{II.43}$$

where $t_\alpha \equiv a_\alpha t$ and $\xi_\alpha \equiv \sigma/2a_\alpha$, then it is clear that the behavior is essentially the same for all of the normal modes; the only difference arises from the time constant $1/a_\alpha$ and the coupling constant ξ_α. Thus, it is sufficient initially to consider only one mode and we can temporarily drop the subscript α. For definiteness and simplicity, we will consider the normal mode of a Hookean dumbbell, for which the normal coordinate is identical with the relative coordinate between the beads.

III. Hookean Dumbbell

The behavior of a Hookean dumbbell is particularly simple to visualize because its only normal mode corresponds to the relative coordinate between the beads. In

addition, the results of the dumbbell can be easily generalized to describe the behavior of an arbitrary normal coordinate of the entire chain. Therefore, in this section we study the behavior of the dumbbell in detail.

As noted in eq II.41, the presence of the shear flow gives rise to a coupling between the x and y directions. A coordinate rotation cannot remove this coupling; it will, however, make the SE easier to solve. Therefore, we rotate the coordinates about the z axis through an angle defined by

$$\tan(2\theta) = 1/\xi \tag{III.1}$$

and then introduce scaling factors, so that the new coordinates are defined by

$$\begin{aligned} x' = Q_x' &= 2\sin\theta(\Theta\cdot Q)_x \\ y' = Q_y' &= 2\cos\theta(\Theta\cdot Q)_y \\ z' = Q_z' &= (\Theta\cdot Q)_z \end{aligned} \tag{III.2}$$

where

$$\Theta = \begin{pmatrix} \cos\theta & \sin\theta & 0 \\ -\sin\theta & \cos\theta & 0 \\ 0 & 0 & 1 \end{pmatrix} \tag{III.3}$$

In terms of these coordinates, the equation of motion for ϕ is

$$\partial_t\phi = [2\sin^2\theta(\partial_{x'}^2 + x'\partial_{x'}) + 2\cos^2\theta(\partial_{y'}^2 + y'\partial_{y'}) + (\partial_{z'}^2 + z'\partial_{z'}) - \cos(2\theta)(y'\partial_{x'} - x'\partial_{y'}) + 3]\phi \tag{III.4}$$

The time-independent solution is a simple Gaussian:

$$\phi_0 = J_0\exp[-\tfrac{1}{2}(x'^2 + y'^2 + z'^2)] = J_0\exp[-\tfrac{1}{2}\vec{Q}'\cdot\vec{Q}'] \tag{III.5}$$

(This solution is identical with that given in eq II.42 but is expressed in term of the new coordinates.) The coupling between x and y does not appear in the time-independent solution. The coordinate rotation angle, θ, was chosen so that the x and y axes lie along the symmetry axes of the distribution function. The lengths were then rescaled so that the steady-state distribution function would have spherical symmetry.

We now seek the time-dependent solutions to eq III.4, following a procedure analogous to that used to study the equilibrium problem. That is, we define a new function ψ by

$$\phi = \psi_0\psi \tag{III.6}$$

where ψ_0 is defined in terms of the steady-state distribution ϕ_0:

$$\phi_0 \equiv \psi_0^2 \tag{III.7}$$

The equation of motion for the wave function ψ is

$$\partial_t\psi = [2\sin^2\theta(\partial_{x'}^2 - \tfrac{1}{4}x'^2 + \tfrac{1}{2}) + 2\cos^2\theta(\partial_{y'}^2 - \tfrac{1}{4}y'^2 + \tfrac{1}{2}) + (\partial_{z'}^2 - \tfrac{1}{4}z'^2 + \tfrac{1}{2}) - \cos(2\theta)(y'\partial_{x'} - x'\partial_{y'})]\psi \equiv S\psi \tag{III.8}$$

Were it not for the last term on the right, the operator S would have the same form as the corresponding operator in equilibrium, given in eq II.34, which can be recovered by setting $\theta = \pi/4$. Two points are to be made regarding the last term. First, it describes the coupling between the x' and y' directions. That this coupling does not appear in the NESS distribution function in eq III.5 implies that only dynamical (time dependent) properties are affected. Second, the last term in non-Hermitian. Therefore, we cannot seek an eigenfunction solution before investigating the properties of the operator S further.

Bose Operator Representation. Rather than studying S in its present form, given in eq III.8, we find it useful to develop a Bose operator representation of S.[16] The specific representation used here is that of Guyer.[17] Define the three-component Bose operators $\vec{B}$ and $\vec{B}^\dagger$ by

$$\begin{aligned} \vec{B} &= \frac{\partial}{\partial\vec{Q}'} + \tfrac{1}{2}\vec{Q}' \\ \vec{B}^\dagger &= -\frac{\partial}{\partial\vec{Q}'} + \tfrac{1}{2}\vec{Q}' \end{aligned} \tag{III.9}$$

which have the property $[\vec{B}, \vec{B}^\dagger] = \mathbf{I}$. ($B_i^\dagger$ is a creaction operator, B_i is a destruction operator, and $B_i^\dagger B_i$ is the number operator.) In terms of these Bose operators, we have (dropping the primes on the subscripts)

$$S = \vec{B}^\dagger\cdot\vec{B} - \cos(2\theta)[(B_x^\dagger B_x - B_y^\dagger B_y) + (B_x^\dagger B_y - B_y^\dagger B_x)] \tag{III.10}$$

In equilibrium ($\theta = \pi/4$), the eigenstates of S are the quantum oscillator states $|(lmn)\rangle$, where l, m, and n are the occupation numbers corresponding to x', y', and z', respectively.

The most immediately important property of S is that it is a nonnormal operator (i.e., $[S, S^\dagger] \neq 0$). Consequently, it *cannot* be diagonalized and does *not* possess a complete set of eigenstates.[18] A second important property of S is that it is number preserving. That is, an excitation is never created without the simultaneous destruction of another excitation. Since the z' direction is not coupled to x' and y', the number of z' excitations is not altered by the action of S. In fact, behavior in the z' direction is completely unaffected by the presence of the flow.

Solution to the Diffusion Equation. As in equilibrium, the formal solution to the diffusion equation (III.8) is

$$\psi(t) = \exp(-St)\psi(0) \tag{III.11}$$

ψ cannot be expanded in eigenfunctions of S, the procedure employed for equilibrium, because S does not have a complete set of eigenfunctions. Nevertheless, a more practical and illuminating form of the solution can be obtained by expanding ψ in terms of the harmonic oscillator basis functions, i.e., eigenfunctions of $\vec{B}^\dagger\cdot\vec{B}$. In ket notation

$$|\psi(t)\rangle = \exp(-St)|\psi(0)\rangle \tag{III.12}$$

and

$$|\psi(t)\rangle = \sum_{lmn=0}^{\infty} C_{lmn}(t)|(lmn)\rangle \tag{III.13}$$

The expansion coefficients $C_{lmn}(t)$ are determined by the matrix equation

$$C_{lmn}(t) = \langle lmn|e^{-St}|l'm'n'\rangle C_{l'm'n'}(0) \qquad \text{(sum implied)} \tag{III.14}$$

Normalization requires that $\langle 0|\psi(t)\rangle = 1$, and therefore $C_{000}(t) = 1$ for all times.

It is convenient to separate S into an equilibrium term S_0 and a flow-dependent term F:

$$S = S_0 + F \tag{III.15a}$$

$$S_0 = \vec{B}^\dagger\cdot\vec{B} \tag{III.15b}$$

and

$$F = -\cos(2\theta)[(B_x^\dagger B_x - B_y^\dagger B_y) + (B_x^\dagger B_y - B_y^\dagger B_x)] \tag{III.15c}$$

Since $[S_0, F] = 0$, we have that

$$e^{-St} = e^{-S_0 t}e^{-Ft} \tag{III.16}$$

and, therefore, for eq III.14, we have

$$C_{lmn}(t) = e^{-Lt}\langle lmn|e^{-Ft}|l'm'n'\rangle C_{l'm'n'}(0) = e^{-Lt}\langle lm|e^{-Ft}|l'm'\rangle C_{l'm'n}(0) \quad \text{(III.17)}$$

where $L = l + m + n$ is the total number of excitations. Since F is function only of x and y, we have introduced the two-dimensional ket $|lm\rangle$, which is in the subspace of x and y excitations. Since many of the calculations that follow will be concerned only with this subspace, we introduce M to play the two-dimensional role of L. That is, $M = l + m$. We also use M to represent the set of occupation numbers (lm).

We define the matrix

$$T_M{}^{M'} = T_{lm}{}^{l'm'} = \langle lm|e^{-Ft}|l'm'\rangle \quad \text{(III.18)}$$

Then, eq III.17 can be written compactly as

$$C_{lmn}(t) = e^{-Lt}T_{lm}{}^{l'm'}C_{l'm'n}(0) \quad \text{(III.19)}$$

$e^{-Lt}T_{lm}{}^{l'm'}$ is the time evolution operator e^{-St}, expressed in the number representation of the harmonic oscillator.

Exponentiation of the Operator F. To find $T_M{}^{M'}$, we need the matrix form of the exponential of the operator $-Ft$. By definition, this is the same as the exponential of the matrix form of the operator $-Ft$. Thus, we need to exponentiate the matrix $-t\mathbf{F}$, whose elements are defined by

$$F_M{}^{M'} = \langle M|F|M'\rangle \quad \text{(III.20)}$$

Using eq III.15c and the Bose algebra defined by

$$B^\dagger|\alpha\rangle = (\alpha + 1)^{1/2}|(\alpha + 1)\rangle \quad \text{(III.21a)}$$

and

$$B|\alpha\rangle = \alpha^{1/2}|(\alpha - 1)\rangle \quad \text{(III.21b)}$$

we find that

$$\langle lm|F|l'm'\rangle = -\cos(2\theta)\{(l - m)\delta_{ll'}\delta_{mm'} + [(lm')^{1/2}\delta_{l,l'+1}\delta_{m,m'-1} - (l'm)^{1/2}\delta_{l,l'-1}\delta_{m,m'+1}]\} \quad \text{(III.22)}$$

If the rows and columns of F are labeled in blocks according to the total number of x and y excitations, then F is block diagonal, having blocks of dimension $M + 1$. This labeling is depicted in Figure 4.

Each block in a block diagonal matrix does not interact with the others. Therefore, the various blocks in $\mathbf{F}$ can be exponentiated independently. The blocks are specified by the total number of x and y excitations, M. Consequently, within a given block, it is only necessary to specify either the number of x excitations or the number of y excitations. (These features follow directly from the number-preserving nature of F.) This suggests an alternative, but equivalent and more convenient, way to label the rows and columns of $\mathbf{F}$, which is to specify M and (without loss of generality) l rather than l and m. This labeling is also included in Figure 4 (under the heading "block row no."). Note that by having the row numbers begin with zero rather than one, they correspond to the number of x excitations. In this notation, we have

$$\langle lm|F|l'm'\rangle = \langle l,M-l|F|l',M'-l'\rangle = \langle l,M-l|F|l',M-l'\rangle\delta_{MM'} = (F_M)_l{}^{l'}\delta_{MM'} \quad \text{(III.23)}$$

$\mathbf{F}_M$ is the $(M + 1)$-dimensional matrix corresponding to the Mth block. From eq III.22, we have

$$(F_M)_l{}^{l'} = -\cos(2\theta)[(2l - M)\delta_{ll'} + ((l' + 1) \times (M - l'))^{1/2}\delta_{l,l'+1} - ((l + 1)(M - l))^{1/2}\delta_{l,l'-1}] \quad \text{(III.24)}$$

The matrices we need to exponentiate are those defined by eq III.24. In Appendix A, we show that $\mathbf{F}_M$ is a nilpotent matrix of index $M + 1$; i.e.

$$(\mathbf{F}_M)^{M+1} = 0 \quad \text{(III.25)}$$

Therefore, using the series expansion of e^x, the exponential of F_M can be written as a *finite* sum of powers of $\mathbf{F}_M$. Thus

$$\exp(-\mathbf{F}_M t) = \sum_{i=0}^{M}\frac{1}{i!}(-t)^i(\mathbf{F}_M)^i \quad \text{(III.26)}$$

and

$$\langle l,M-l,n|e^{-Ft}|l',M'-l',n'\rangle = \delta_{nn'}\delta_{MM'}\sum_{i=0}^{M}\frac{1}{i!}(-t)^i\langle l,M-l|F|l',M-l'\rangle \quad \text{(III.27)}$$

We can use the foregoing results to rewrite the solution for the wave function given in eq III.13 and III.14:

$$|\psi(t)\rangle = \sum_{n,m=0}^{\infty}\sum_{l=0}^{M}C_{l,M-l,n}(t)|l,M-l,n\rangle \quad \text{(III.28a)}$$

where

$$C_{l,M-l,n}(t) = e^{-Lt}\sum_{l'=0}^{M}(T_M)_l{}^{l'}C_{l',M-l',n}(0) \quad \text{(III.28b)}$$

and

$$(T_M)_l{}^{l'} = \sum_{i=0}^{M}\frac{1}{i!}(-t)^i\langle l,M-l|F^i|l',M-l'\rangle \quad \text{(III.28c)}$$

This is the simplest form into which the solution can be cast unless the transformation that puts $\mathbf{F}_M$ into Jordan canonical form is known. For many quantities of interest, only small values of M contribute and T can be determined explicitly.

To understand the behavior described by eq III.28, let us suppose that initially a specific excited state of the system is occupied; say, for example, the state $|l,K-l,j\rangle$. That is

$$C_{l',M-l',n}(0) = \delta_{l',l}\delta_{M,K}\delta_{nj} + \delta_{l',0}\delta_{M,0}\delta_{n,0} \quad \text{(III.29)}$$

(The second term in $C(0)$ is required for normalization of the probability distribution.) The state of the system at later times is

	no. of excitations M dimension d	row no.	block row no.	(lm)
0th block	$M = 0$			
	$d = 1$	1	0	(00)
1st block	$M = 1$	2	0	(01)
	$d = 2$	3	1	(10)
2nd block	$M = 2$	4	0	(02)
	$d = 3$	5	1	(11)
		6	2	(20)
3rd block	$M = 3$	7	0	(03)
	$d = 4$	8	1	(12)
		9	2	(23)
		10	3	(34)
		⋮		

Figure 4. Labeling of the matrix F. The matrix F is block diagonal. The zeroth block is 1×1 and acts on states in which there are neither x' nor y' excitations; the first block is 2×2 and acts on states having either one x' or one y' excitation; the third block is 3×3 and acts on states having two x' or y' excitations; etc. If the rows and columns of the block matrices are labeled $0 \rightarrow M$, where M is the total number of x' and y' excitations, then the row and column numbers correspond to the number of x' excitations. This labeling is given in the fourth column of the figure.

$$|\psi(t)\rangle = |0\rangle + \sum_{l'=0}^{K} e^{-(K+j)t}(T_K)_l^{l'}|l',K-l',j\rangle \quad \text{(III.30)}$$

The total number of excitations will not change, though their amplitude will decay with the overall factor $e^{-(K+j)t}$. As time evolves, however, the K excitations in the x and y subspace will be redistributed. The states $|l\pm i,K-l\mp i,j\rangle$ will begin to grow with an initial time dependence t^i. The time dependence is an exponential modified by a polynomial in t, rather than purely exponential decay. Eventually, the exponential factor will dominate and all states will decay (except $|0\rangle$, of course).

It is appropriate to point out here that each matrix $\mathbf{F}_M$ does have one (and only one) eigenvector, whose eigenvalue vanishes. That eigenvector is

$$|M\rangle = \sum_{l=0}^{M}(-1)^l\left[\frac{M!}{2^M l!(M-l)!}\right]^{1/2}|l,M-l\rangle \quad \text{(III.31)}$$

If there are no excitations in the z direction, then this eigenvector corresponds to a distribution function in *laboratory* coordinates

$$\phi_M = J_M H_M(\zeta)\phi_{ss}$$
$$\zeta = \frac{x - 4\xi y}{2^{1/2}[1 + \xi^2]^{1/2}} \quad \text{(III.32)}$$

where H_M is the Mth Hermite polynomial. If one of the eigenstates of the system is excited, then the decay back to steady state will be purely exponential.

Results. Despite the somewhat cumbersome form of the solution to the diffusion equation, appearing in eq III.28, we can nevertheless determine some quantities of interest. In particular, we consider the position correlation functions.

An arbitrary correlation function, in the rotated coordinate system, is given by

$$\langle f(t)g(0)\rangle = \langle 0|fe^{-St}g|0\rangle = \sum_{n,n'=0}^{\infty}\sum_{M,M'=0}^{\infty}$$
$$\sum_{l,l'=0}^{MM'}\langle 0|f|l,M-l,n\rangle\langle l,M-l,n|e^{-Ft}|l',M'-l',n'\rangle = \sum_{n,M=0}^{\infty}$$
$$\sum_{l,l'=0}^{M} e^{-(M+n)t}\langle 0|f|l,M-l,n\rangle\langle l,M-l|e^{-Ft}|l',M-l'\rangle\langle l',M-l',n|g|0\rangle \quad \text{(III.33)}$$

We can evaluate the position correlation function by taking f and $g = \vec{Q}' = \vec{B}^\dagger + \vec{B}$. We need to determine only $\exp(-t\mathbf{F}_0)$ and $\exp(-t\mathbf{F}_1)$. From eq III.24, we find

$$\exp(-t\mathbf{F}_0) = \mathbf{I}$$
$$\exp(-t\mathbf{F}_1) = \mathbf{I} - t\mathbf{F}_1 \quad \text{(III.34)}$$

where

$$\mathbf{F}_1 = \cos(2\theta)\begin{pmatrix} 1 & 1 \\ -1 & -1 \end{pmatrix}$$

The correlation functions in the rotated coordinate system are

$$\langle z'(t)z'(0)\rangle = e^{-t}$$
$$\langle y'(t)y'(0)\rangle = e^{-t}(1 - t\cos(2\theta))$$
$$\langle x'(t)x'(0)\rangle = e^{-t}(1 + t\cos(2\theta))$$
$$\langle x'(t)y'(0)\rangle = e^{-t}(-t\cos(2\theta)) \quad \text{(III.35)}$$
$$\langle y'(t)x'(0)\rangle = e^{-t}(2t\cos(2\theta))$$
$$\langle z'(t)y'(0)\rangle = \langle y'(t)z'(0)\rangle = 0$$
$$\langle z'(t)x'(0)\rangle = \langle x'(t)z'(0)\rangle = 0$$

These results can be transformed back to the laboratory frame by using the definitions in eq III.1 to III.3. The results in matrix form are

$$\langle\vec{R}^*(t)\vec{R}^*(0)\rangle = e^{-t}\begin{pmatrix} (1 + 2\xi^2 + 2\xi^2 t) & \xi(1+2t) & 0 \\ \xi & 1 & 0 \\ 0 & 0 & 1 \end{pmatrix} \quad \text{(III.36)}$$

(More correctly, we seek $\langle\vec{R}^*(t)\vec{R}^*(t')\rangle$, which is given by eq III.36 if t is replaced by $|t - t'|$.) The order of labeling of the rows and columns i (xyz). For example, $\langle y(t)x(0)\rangle = e^{-t}(\xi)$. At $t = 0$, the results for the average behavior in the steady state, which can be determined directly from the distribution function in eq II.42, are recovered. Referring once more to Figure 2, we note that the distribution is broader in x than in y. This feature is indicated in the correlation functions by the result $\langle x^2\rangle \geq \langle y^2\rangle$. That $\langle xy\rangle \neq 0$ and is positive indicates that x and y are more likely to have the same signs than opposite signs, a feature that is also evident in Figure 2.

The position correlation functions and the anisotropic feature of the distribution function can be understood more fully by studying the time dependence of the correlation functions as the system evolves from a given displacement back to the steady state. That is, we will study the conditional average $\langle f(t|\vec{R}_0^*0)\rangle$, the average value of f at time t given the system is at $\vec{R}_0^* = (x_0,y_0,z_0)$ at $t = 0$, which is given by

$$\langle f(t|\vec{R}_0^*0)\rangle = \int d\vec{R}^*\, f(\vec{R}^*)\phi(\vec{R}^*t|\vec{R}_0^*0) \quad \text{(III.37)}$$

If the system is at $\vec{R}_0^*$ at $t = 0$, then

$$\phi(0) = \delta(\vec{R}^* - \vec{R}_0^*) \quad \text{(III.38)}$$

and

$$\psi(0) = \delta(\vec{R}^* - \vec{R}_0^*)[\psi_0(\vec{R}_0^*)]^{-1/2}$$

Using the closure relation (valid for any complete set of states), we can rewrite the δ function in terms of the eigenfunctions:

$$\delta(\vec{R}^* - \vec{R}_0^*) = \sum_{n,M=0}^{\infty}\sum_{l=0}^{M}\psi_{l,M-l,n}(\vec{R}^*)\psi_{l,M-l,n}(\vec{R}_0^*) \quad \text{(III.39)}$$

where $\psi_{l,M-l,n}(\vec{R}^*)$ is the projection of $|l,M-l,n\rangle$ onto $\vec{R}^*$. Explicitly[16]

$$\psi_{l,M-l,n}(\vec{R}^*) = 2^{-(M+n)/2}\left[\frac{1}{l!(M-l)!n!}\right]^{1/2} \times$$
$$H_l\left(\frac{x}{2^{1/2}}\right)H_{M-l}\left(\frac{y}{2^{1/2}}\right)H_n\left(\frac{z}{2^{1/2}}\right)\psi_0(\vec{R}^*) \quad \text{(III.40)}$$

Using the solution given in eq III.28, along with eq III.37 to III-39, we find for the conditional average of an arbitrary function $f(\vec{R}^*)$ at time t

$$\langle f(t|\vec{R}_0^*)\rangle = \sum_{n,M=0}^{\infty}\sum_{l,l'=0}^{M} e^{-(M+n)t}\frac{\psi_{l,M-l,n}(\vec{R}_0^*)}{\psi(\vec{R}_0^*)}\langle 0|f|l',M-l',n\rangle \times$$
$$\langle l',M-l'|e^{-Ft}|l,M-l\rangle \quad \text{(III.41)}$$

The ratio of the wave functions is given by eq III.40.

For the conditional average displacement, only $n,M = 0$ and 1 contribute. Using $H_0(x) = 1$ and $H_1(x) = 2x$, we find, in the *rotated* coordinate system

$$\langle x'(t|\vec{Q}_0'0)\rangle = e^{-t}[(y_0' + x_0')t\cos(2\theta) + x_0']$$
$$\langle y'(t|\vec{Q}_0'0)\rangle = e^{-t}[(y_0' + x_0')(-t\cos(2\theta)) + y_0'] \quad \text{(III.42)}$$
$$\langle z'(t|\vec{Q}_0'0)\rangle = e^{-t}z_0'$$

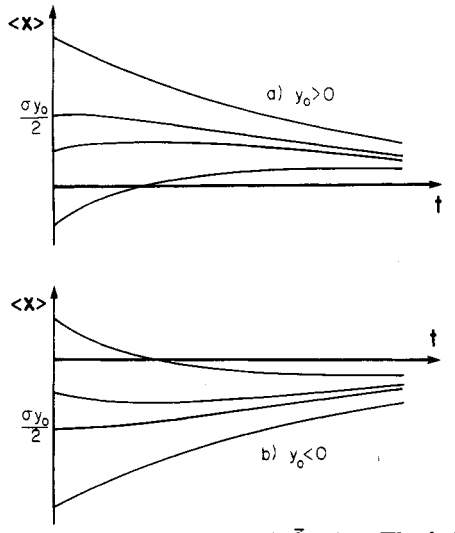

Figure 5. Conditional average $\langle x(t|\vec{R}_0{}^*0)\rangle$. The behavior of $\langle x(t|\vec{R}_0{}^*0)\rangle$ (abbreviated $\langle x(t)\rangle$) is plotted as a function of time. $|\langle x(t)\rangle|$ achieves a maximum whenever $x_0 < |2\xi y_0|$. $\langle x(t)\rangle$ approaches its steady-state value $\langle x(\infty)\rangle = 0$ with the same sign as y_0.

The desired results are obtained by transforming back to the laboratory frame:

$$\langle \vec{R}^*(t|\vec{R}_0{}^*0)\rangle = e^{-t}\begin{pmatrix} x_0 + 2\xi y_0 t \\ y_0 \\ z_0 \end{pmatrix} \qquad \text{(III.43)}$$

The decays of the y and z displacements depend only on the initial displacements y_0 and z_0, respectively. The decay of the x displacement, on the other hand, depends not only upon x_0 but also upon y_0 as time evolves. The coupling parameter is the dimensionless velocity gradient ξ. The behavior of $\langle x(t|\vec{R}_0{}^*0)\rangle$, abbreviated $\langle x(t)\rangle$, is illustrated in Figure 5, for several choices of x_0 and y_0. Note that if $x_0/(2\xi y_0) < 1$, then the magnitude of the x displacement, $|\langle x(t)\rangle|$, can actually increase before decreasing. The maximum will occur at

$$t_{max} = 1 - x_0/(2\xi y_0) \qquad \text{(III.44)}$$

Another interesting feature is that, as the system decays back to the steady state, $\langle x(t)\rangle$ always approaches zero with the same sign as y_0. This behavior is evident in eq III.43; the term $2\xi y_0 t$ will always dominate x_0 after a sufficiently long time. This is not surprising, since we have seen that in the steady state, x and y are more likely to have the same sign than opposite signs.

The effect of the shear flow on the decay of $\langle x(t)\rangle$ and $\langle y(t)\rangle$ back to their steady-state values of zero is seen more dramatically in the parametric plot in Figure 6. This plot shows the trajectory followed by the mean end-to-end vector $\langle \vec{R}^*(t|\vec{R}_0{}^*0)\rangle$, projected onto the (x,y) plane, for several initial displacements. The trajectories are determined by eq III.43 and are given analytically by

$$x = [(x_0/y_0) - 2\xi \ln (y/y_0)]y \qquad \text{(III.45)}$$

If there were no flow ($\xi = 0$), the trajectories would be straight lines from the initial state to the origin. In the presence of a flow, however, the dumbbell rotates to align with the flow as it relaxes back to its steady-state position. Note that if the initial y displacement, y_0, is positive, then the displaced bead is "pushed" to the right by the flow; if y_0 is negative, the displaced bead is "pushed" to the left. This is as one would expect physically (refer to Figure 3). $\langle x(t)\rangle$ achieves a maximum along the line $x = 2\xi y$, which is shown as a dashed line in the figure.

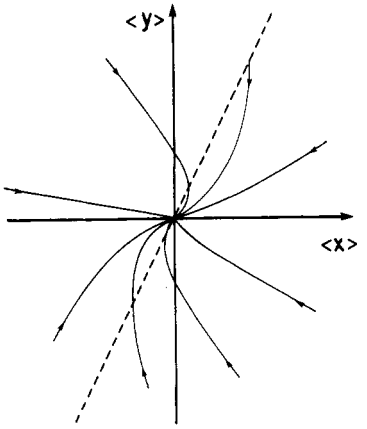

Figure 6. Trajectories of $(\langle x(t)\rangle, \langle y(t)\rangle)$. This is a plot of the mean end-to-end vector $\langle \vec{R}^*\rangle$, projected onto the (x,y) plane, for various initial conditions. The dumbbell aligns with the flow as it relaxes back to its steady state distribution from an initial state.

The conditional average $\langle \vec{R}^*(t|\vec{R}_0{}^*0)\rangle$ in eq III.43 helps us to explain the behavior of the time correlation functions in eq III.36. The correlation functions are obtained by measuring $\vec{R}^*$ at $t = 0$ and again at subsequent times, forming the product $\vec{R}^*(t)\vec{R}^*(0)$, and then averaging this quantity in the steady state. Let us consider this process in light of the conditional average. For a given $\vec{R}_0{}^*$, the subsequent values of y will be, on average, $y(t) = y_0 e^{-t}$. Averaging over the steady state then gives, for example

$$\langle y(t)y(0)\rangle = \langle y_0 y_0\rangle e^{-t}$$
$$\langle y(t)x(0)\rangle = \langle y_0 x_0\rangle e^{-t} \qquad \text{(III.46)}$$

The subsequent values of x, on the other hand, are coupled to y_0 as time evolves. Thus, we have

$$\langle x(t)y(0)\rangle = \langle (x_0 + 2y_0 t)y_0\rangle e^{-t}$$
$$\langle x(t)x(0)\rangle = \langle (x_0 + 2y_0 t)x_0\rangle e^{-t} \qquad \text{(III.47)}$$

This explains the lack of symmetry in the time correlation function $\langle \vec{R}^*(t)\vec{R}^*(0)\rangle$: The time evolution of the x displacement is coupled to the initial y displacement, whereas the evolution of the y displacement is not coupled to the initial x displacement.

From the correlation functions in eq III.36, we can immediately determine the prediction of the Hookean dumbbell model for the stress tensor and the material functions of a dilute solution. These are well-known results;[2] they are given in Appendix B.

The discussion of the Hookean dumbbell model presented here adds to our understanding of the Rouse model in several ways. The intuitive expectation that a stretched dumbbell in shear flow will rotate to become aligned with the flow is confirmed quantitatively. This behavior is depicted most clearly in Figure 6. The advantage of using the dumbbell model to demonstrate this behavior is that the sole normal coordinate corresponds precisely to the end-to-end vector; i.e., it corresponds to the relative coordinate of the beads. Hence, there is no difficulty in transforming from the normal coordinates to laboratory coordinates. The dumbbell model also demonstrates that fluctuations about the steady-state distribution of the dumbbell coordinates do not decay back to the steady state with a purely exponential relaxation. Rather, the relaxation is modified by polynomials in t. The same time dependence arises in Hookean chains, as will be seen in section IV. This additional time dependence is important in predicting the outcome of frequency-dependent measurements which are made on a system undergoing shear.

Having studied the Hookean dumbbell in shear flow fairly exhaustively, we will now proceed to the study of Hookean chains in shear flow.

IV. Harmonic Chains

As noted in section II, all of the results for the Hookean dumbbell are easily extended to the αth normal mode of a harmonic chain by making the replacement $t \rightarrow t_\alpha \equiv a_\alpha t$ and $\xi \rightarrow \xi_\alpha \equiv 2\xi/a_\alpha$. Thus, the behavior of the chain is already understood in terms of its normal modes. The major difficulty in using the normal mode results to describe the chain behavior is a mathematical one—namely, the transformation from normal coordinates to laboratory coordinates. For example, if we want to determine the correlations between different beads, we must sum over the contributions from all normal modes. We will consider three quantities of interest—the position correlation function between different beads, the dynamic structure factor of the chain, and the material functions.

Position Correlation Function. The dimensionless position correlation function $\Delta_{ij}(t)$ is a 3×3 matrix defined by

$$\Delta_{ij} = \langle[\vec{R}_i(t) - \vec{R}_j(0)][\vec{R}_i(t) - \vec{R}_j(0)]\rangle = \langle\vec{R}_i(0)\vec{R}_i(0)\rangle + \langle\vec{R}_j(0)\vec{R}_j(0)\rangle - \langle\vec{R}_i(t)\vec{R}_j(0)\rangle - \langle\vec{R}_j(t)\vec{R}_i(0)\rangle \quad \text{(IV.1)}$$

Using eq II.22 and II.29, we can express the required correlation functions in terms of the normal coordinates:

$$\langle\vec{R}_i(t)\vec{R}_j(0)\rangle = \sum_{\mu\sigma\nu} B_{i\mu}^{-1}B_{j\sigma}^{-1}U_{\mu\nu}U_{\sigma\nu}\langle\vec{Q}_\nu(t)\vec{Q}_\nu(0)\rangle \quad \text{(IV.2)}$$

We have used the independence of the normal coordinates, that is, that $\langle\vec{Q}_\alpha(t)\vec{Q}_\alpha(0)\rangle \propto \delta_{\alpha\beta}$. Using the dumbbell results in eq III.36, we can infer that

$$\langle\vec{Q}_\alpha(t)\vec{Q}_\alpha(0)\rangle \begin{pmatrix} 1 + \frac{8\xi^2}{a_\alpha^2}(1 + a_\alpha t) & \frac{2\xi}{a_\alpha}(1 + 2a_\alpha t) & 0 \\ \frac{2\xi}{a_\alpha} & 1 & 0 \\ 0 & 0 & 1 \end{pmatrix} \quad \text{(IV.3)}$$

Only the xx, xy, and yx components of Δ_{ij} are affected by the flow; thus

$$(\Delta_{ij})_{xz} = (\Delta_{ij})_{zx} = 0$$
$$(\Delta_{ij})_{yz} = (\Delta_{ij})_{zy} = 0 \quad \text{(IV.4)}$$
$$(\Delta_{ij})_{yy} = (\Delta_{ij})_{zz} = \tfrac{1}{3}\Delta^\circ_{ij}$$

Δ°_{ij} is the equilibrium ($\xi = 0$) correlation function given by

$$\Delta^\circ_{ij}(t) = \langle[\vec{R}_i(t) - \vec{R}_j(0)]^2\rangle_0 = 3\sum_{\mu\sigma\nu}[B_{i\mu}^{-1}B_{i\sigma}^{-1} + B_{j\mu}^{-1}B_{j\sigma}^{-1} - 2B_{i\mu}^{-1}B_{j\sigma}^{-1}e^{-a_\nu t}]U_{\mu\nu}U_{\sigma\nu} \equiv 3\sum_{\mu\sigma\nu} S_{ij}(\mu,\nu,\sigma;t) \quad \text{(IV.5)}$$

We also define

$$\Delta_1(ij,t) = \sum_{\mu\sigma\nu}\frac{1}{a_\nu}S_{ij}(\mu,\sigma,\nu;t)$$

and

$$\Delta_2(ij,t) = \sum_{\mu\sigma\nu}\frac{1}{a_\nu^2}S_{ij}(\mu,\sigma,\nu;t) \quad \text{(IV.6)}$$

In terms of these sums, the interesting components of $\Delta_{ij}(t)$ are, from eq IV.3,

$$(\Delta_{ij})_{xx} = \tfrac{1}{3}\Delta^\circ_{ij} + 8\xi^2[\Delta_2(ij,t) + t\Delta_1(ij,t)]$$
$$(\Delta_{ij})_{xy} = 2\xi[\Delta_1(ij,t) + \tfrac{2}{3}t\Delta^\circ_{ij}] \quad \text{(IV.7)}$$
$$(\Delta_{ij})_{yx} = 2\xi\Delta_1(ij,t)$$

The sums in eq IV.5 and IV.6 are evaluated for large N in detail in ref 20 and in summary in Appendix C. The results are valid only for $t \ll N^2$ and $N \gg 1$. (These inequalities specify what is meant by "large" N.) A feature worth noting, which arises in shear flow but is absent in equilibrium, is that the mean square bead separation depends not only on the separation of the beads along the chain ($i - j$) but also on the chain length. This feature can be understood in two ways. First, longer chains probe longer distances and therefore experience greater velocity differences. Consequently, they are distorted by the flow more than short chains. Second, the greatest contributions to the separation are from the long-wavelength, low-lying modes. As was discussed previously, in section II, these modes are more strongly coupled to the flow; furthermore, the coupling is stronger for longer chains. The general results for the correlation function are cumbersome and not very illuminating (see ref 20 and Appendix C); we will, however, consider several interesting limits.

The correlations between the 1st and the $(N + 1)$st beads determine the average behavior of the end-to-end vector R. Recalling that we may consider only $t \ll N^2$, the correlation functions are

$$\langle R_xR_x\rangle = N[1 + \tfrac{1}{15}\xi^2N^4(1 + 8t/3N^2 + ...)]$$
$$\langle R_xR_y\rangle = \tfrac{1}{6}\xi N^3(1 + 5t/36N^2 + ...)$$
$$\langle R_yR_x\rangle = \tfrac{1}{6}\xi N^3(1 - t/36N^2 + ...)$$
$$\langle R_yR_y\rangle = \langle R_zR_z\rangle = N \quad \text{(IV.8)}$$

These results agree with an earlier calculation of $\langle R^2\rangle$ at $t = 0$.[9,19] The dependence on N seen here can be understood by the following argument. In the steady state, the net force acting on the chain must vanish. Thus, the spring forces that act to coil the chain and the friction forces that act to stretch the chain must balance. The friction force that stretches the chain is

$$\zeta\dot{\gamma}\sum_1(y_{i+1} - y_i)\hat{x} = \zeta\dot{\gamma}(y_{N+1} - y_1)\hat{x} = \zeta\dot{\gamma}R_y\hat{x}$$

The harmonic force acting to coil the chain is given by the product of the amplitude of an eigenvector and the eigenfrequency. In terms of the normal coordinates, the force for the νth mode is $\vec{F}_\nu = a_\nu\vec{Q}_\nu$. The softest normal mode, which is the most easily excited, is the lowest mode ($\nu = 1$). Its frequency is $a_1 \sim N^{-2}$. It has no nodes, and therefore its amplitude goes as $\vec{R}$. Equating these forces gives

$$\Gamma N^{-2}R_x \sim \zeta\dot{\gamma}R_y$$

or

$$R_x \sim \xi N^2R_y$$

Thus, $\langle R_xR_y\rangle \sim N^2\langle R_yR_y\rangle \sim \xi N^3$. This argument also accounts for the second term in $\langle R_xR_x\rangle$, since

$$\langle R_xR_x\rangle \sim N^4\xi^2\langle R_yR_y\rangle \sim \xi^2N^5$$

Next, we consider the self-correlation function $\Delta_{ii}(t)$. We consider a bead near the center of the chain, that is, $i \sim N/2$, for which end effects are unimportant. In this limit, one can show that[20]

$$(\Delta_{ii})_{xx} = 2\left(\frac{t}{\pi}\right)^{1/2} + \frac{\xi^2}{45}tN^3$$

$$(\Delta_{ii})_{xy} = (\Delta_{ii})_{yx} = \frac{\xi}{3}tN \qquad \text{(IV.9)}$$

This behavior can be understood by an argument similar to that of de Gennes[21] for a chain in equilibrium. The average distance between two beads near the center of the chain in shear flow is given by[20]

$$\langle (x_i - x_j)^2 \rangle = |i - j| + \tfrac{1}{6}\xi^2 N^3 (i - j)^2$$

$$\langle (x_i - x_j)(y_i - y_j) \rangle = \tfrac{1}{2}\xi N (i - j)^2 \qquad \text{(IV.10)}$$

This is the physical distance between two beads separated by a distance $|i - j|$ *along* the chain. In time t, a disturbance can propagate a distance $(i - j)^2$ along the chain. (The fluctuations "random walk" *along* the chain.) In other words, it can travel a distance $|i - j|$ in time $t^{1/2}$. From eq IV.10, this corresponds to a physical distance in space

$$x^2 \sim t^{1/2} + \xi^2 N^3 t$$

and

$$xy \sim \xi N t$$

Structure Factor. The dynamic structure factor for a harmonic chain can be determined directly from the correlation function $\Delta_{ij}(t)$. The structure factor is defined as

$$S(\vec{k},t) = \frac{1}{N}\sum_{ij}\langle e^{i\vec{k}\cdot\vec{R}_i^*(t)} e^{-i\vec{k}\cdot\vec{R}_j^*(0)} \rangle \qquad \text{(IV.11)}$$

Using a cumulant expansion,[22] one can write ln $[S(\vec{k},t)]$ as a power series in $\vec{k}$. Since the steady-state distribution function has a Gaussian form, only the second-order term is nonvanishing. One finds

$$S(\vec{k},t) = \frac{1}{N}\sum_{ij}\exp(-\vec{k}\cdot\Delta_{ij}(t)\cdot\vec{k}) \qquad \text{(IV.12)}$$

To lowest order in $\vec{k}$

$$S(\vec{k},t) = N - \frac{1}{2N}\sum_{ij}\vec{k}\cdot\Delta_{ij}(t)\cdot\vec{k} \qquad \text{(IV.13)}$$

Using the approximation

$$\sum_{n=1}^{N} n^j \sim N^{j+1} \qquad \text{for } N \gg 1$$

one can show

$$\sum_{ij}\Delta_0(ij,0) \sim N^3$$

$$\sum_{ij}\Delta_1(ij,0) \sim N^5$$

and

$$\sum_{ij}\Delta_2(ij,0) \sim N^7$$

Therefore, apart from precise coefficients, the static structure factor to lowest order in $\vec{k}$ is

$$S(\vec{k},0) \sim N\{1 - N[k_x^2(1 + \xi^2 N^4) + 2k_x k_y \xi N^2 + k_y^2 + k_z^2] \sim N(1 - \vec{k}\cdot\langle\vec{R}\vec{R}\rangle\cdot\vec{k}) \qquad \text{(IV.14)}$$

(The latter statement in eq IV.14 is seen by comparison with eq IV.8.) Thus, as in equilibrium, at small wavenumber k, the structure factor probes the coil size. In shear flow, the coil size is anisotropic; the anisotropy increases with increasing velocity gradient and increasing chain length. Very strong dependence is seen in ΔS, the difference between the structure factor in shear flow and in equilibrium:

$$\Delta S(\vec{k},0) \sim -N(\xi^2 N^4 k_x^2 + 2\xi N^2 k_x^2 k_y^2) \qquad \text{(IV.15)}$$

The static structure factor can be used to obtain information about the length of a polymer chain. The dependence of $S(\vec{k},0)$ on length is much stronger in shear flow than in equilibrium. The dynamic structure factor is also modified by the shear flow, not only in its dependence on chain length but also in its time dependence, and is given by eq IV.13.

Material Functions. The prediction of the Rouse model for the material functions of a dilute solution can be found easily from the steady-state correlation function. The polymer contribution to the stress tensor of a dilute solution of Rouse chains is[2]

$$\tau_p = nkT[-\sum_i \langle \vec{R}_i^* \vec{R}_i^* \rangle + N\mathbf{I}] \qquad \text{(IV.16)}$$

Using

$$\sum_i \langle \vec{R}_i^* \vec{R}_i^* \rangle = \sum_i \langle \vec{Q}_i \vec{Q}_i \rangle,$$

eq IV.3, and $a_i \simeq (N/\pi i)^2$ leads to the results

$$\eta - \eta_s = nkTN^2\tau/12$$

$$\Psi_1 = nkTN^4\tau^2/180 \qquad \text{(IV.17)}$$

$$\Psi_2 = 0$$

These are the well-known material functions predicted by the Rouse model.[2] The model fails to predict the observed non-Newtonian behavior of the material functions.

V. Conclusion

We have studied and thoroughly understood the behavior of a Hookean dumbbell in steady shear flow. For a given initial fluctuation of the dumbbell out of the nonequilibrium steady state, we have determined the relaxation back to the steady state exactly. The relaxation is altered (with respect to equilibrium) by the presence of shear flow. The degree to which it is altered increases with the size of the fluctuation in the y displacement. Physically, this is because if the beads probe larger distance scales in the y direction, then they sense greater differences in the solvent velocity; consequently, the rotation of the dumbbell by shear flow is stronger. See Figure 6.

We have also determined the exact behavior of the normal modes of a Hookean chain in shear flow. Behavior analogous to that of the dumbbell is obtained. Longer chains, which probe larger distance scales, experience greater coupling to the solvent velocity. Similarly, long-wavelength excitations of the chain, corresponding to the low-lying normal modes, are more strongly coupled to the solvent velocity than are short-wavelength excitations. An arbitrary fluctuation of the chain can be written as a superposition of normal modes; its evolution in time is then known in terms of the evolution of the normal mode contributions.

Generality of the Results. The diffusion operator for a flexible chain in equilibrium can be cast into a Hermitian form, regardless of the spring potential between the beads; see, for example, eq II.10. In this form, the diffusion operator has a complete set of eigenfunctions, which correspond to excitations (or fluctuations) of the distribution function. It follows that the evolution of a given excitation is exponential in time. For the Hookean chain in shear flow, however, we have seen that the exponential relaxation is modified by polynomials in time. This is a general result

which we will now show is true for a chain in shear flow for any spring potential.

The diffusion operator for shear flow cannot be cast into Hermitian form (unless one employs a rotating set of coordinates, which leads to a time-dependent effective potential). Furthermore, it is a nonnormal operator, by virtue of the flow term, and hence cannot be diagonalized. However, for any operator, there exists a complete set of basis states in which its matrix form has Jordan canonical form.[23] This form is block diagonal. Each block has an eigenvalue on the diagonal and zeroes and ones on the superdiagonal (or the subdiagonal). Therefore, the time development operator $\exp(-St)$ is also block diagonal, with each block having the following form:

$$e^{-\lambda t}\begin{pmatrix} 1 & t & t^2/2! & t^3/3! & \dots & t^N/N! \\ 0 & 1 & t & t^2/2! & \dots & t^{N-1}/(N-1)! \\ \cdot & \cdot & \cdot & \cdot & & \cdot \\ \cdot & \cdot & \cdot & \cdot & & \cdot \\ \cdot & \cdot & \cdot & \cdot & & \cdot \end{pmatrix}$$

where λ is the eigenvalue and N is the dimension of the block. The basis states correspond to statistical fluctuations out of the steady state. From the above form of the diffusion operator, we can conclude that, in general, different fluctuations are coupled; the coupling is governed by a polynomial evolution in time, though the overall relaxation is still exponential. These features were evident in the dynamical behavior of the Hookean dumbbell and chains in shear flow.

Modified Gaussian Theories. Our results for the fluctuations of a Hookean chain in shear flow can be applied immediately to modified Gaussian theories, in which nonlinear springs are replaced by Hookean springs with shear rate dependent spring constants; i.e., $\Gamma \rightarrow \Gamma(\dot\gamma)$. The spring constant increases with increasing shear rate and thereby prevents the springs from stretching indefinitely. This gives rise to a non-Newtonian viscosity, a result that can be seen by the following argument: For a non-Hookean spring, the stress tensor is[2]

$$\tau_p = n\{\sum \langle \vec{F}_i \vec{R}_i^* l\rangle + kTN\mathbf{I}\}$$

and therefore

$$\eta - \eta_s = -\frac{n}{\dot\gamma}\langle F_{ix} R_{iy}^*\rangle \qquad \text{(V.1)}$$

where F_i is the force on the ith bead due to the springs. In the steady state, the force exerted by the springs and the force due to the friction must cancel. Thus

$$F_{ix} = -\zeta\dot\gamma l R_{iy}^*$$

for any spring potential. Using $\sum_i R_{iy}^* R_{iy}^* = \sum_i Q_{iy} Q_{iy}$, the viscosity can be written

$$\eta - \eta_s = \zeta l^2 \sum_i \langle Q_{iy} Q_{iy}\rangle \qquad \text{(V.2)}$$

In general, therefore, the viscosity is proportional to the mean square y displacement of the springs. For a modified Gaussian theory, eq V.2 leads to

$$\eta - \eta_s = n\frac{\zeta}{\Gamma(\dot\gamma)}\sum_i \frac{1}{2a_i} \qquad \text{(V.3)}$$

where a_i is the ith Rouse eigenvalue. The viscosity decreases as the shear rate and the spring constant increase. The physical process is this: The shear flow stretches the spring in the x direction. If the nonlinear part of the spring potential becomes important, then the restoring force of the spring is greater than it would be for a Hookean spring. In the x direction, this restoring force is countered by the frictional force of the solvent. However, because of the nonlinearity of the spring force, the increased separation of the beads in the x direction also increases the restoring force in the y direction. Since there is no other force to counter this process, the mean square bead separation y^2 decreases. The viscosity is thereby reduced. The modified Gaussian theories mimic the nonlinear increase in the restoring force of the spring by increasing the Hookean spring constants. Therefore, all of our results for the dynamical fluctuations of a Hookean chain are immediately applicable to modified Gaussian theories. Once the modified spring constant $\Gamma(\dot\gamma)$ has been determined (which can be done by using the steady state), then the fluctuations around the steady state are described by making the replacement $\Gamma \rightarrow \Gamma(\dot\gamma)$. This prescription implicitly assumes that the modified spring constant would not be altered by the dynamics, which is reasonable at least as a first approximation.

Hydrodynamic Interaction. Some of our results are also valid when preaveraged hydrodynamic interactions are included in the model, which, to be consistent, should be preaveraged in the steady state rather than in equilibrium.[12] To include the preaveraged hydrodynamic interactions, the Rouse matrix, the Rouse eigenvalues, and the Rouse normal modes must all be replaced by their Zimm counterparts. With those replacements, the correlation function of the Zimm normal coordinates is given by eq IV.3. The time evolution is like that of the free-draining chain—it is described by exponentials modified by a linear term. The relaxation time and the strength of the coupling to the flow are altered, and therefore the time dependence of the bead correlation function $\Delta_{ij}(t)$ would also change. The precise dependence would be determined by the diagonalizing transformation and the Zimm eigenvalues.

Acknowledgment. The author thanks R. A. Guyer for many useful and stimulating discussions and suggestions and acknowledges B. R. Reinhold for assistance in preparing Figure 2. This work was supported by the National Science Foundation (Grant DMR 8205352) and the Army Research Office (Contract DAAG 29-81-K-0179).

Appendix A

We show here that the matrix $\mathbf{F}_M$, given by eq III.24, is a nilpotent matrix of index $M+1$; i.e., $(\mathbf{F}_M)^{M+1} = 0$. We begin by showing that all eigenvalues of $\mathbf{F}_M$ vanish. To this end, we note that if λ_i ($i = 1, \dots, N+1$) represents the eigenvalues of any $(N+1)$-dimensional matrix $\mathbf{A}$, then

$$\sum_{i=1}^{N+1} \lambda_i^2 = \mathrm{Tr}\ \mathbf{A}^2 \qquad \text{(A.1)}$$

where Tr = trace. One can show that $\mathrm{Tr}\ \mathbf{F}_M{}^2 = 0$. Thus, the sum of the squares of the eigenvalues of $\mathbf{F}_M$ vanishes, which implies that each eigenvalue must vanish. Note that this is true whether or not the eigenvalues are complex, for if λ_i is a complex eigenvalue, then so it λ_i^*; since $(\lambda_i^2 + \lambda_i^{*2}) = (\mathrm{Re}\ \lambda_i)^2 + (\mathrm{Im}\ \lambda_i)^2$, both the real and imaginary parts of λ_i must vanish. From this we can infer that the characteristic equation for $\mathbf{F}_M$, given by

$$\mathrm{Det}\ (\mathbf{F}_M - \lambda\mathbf{I}) = 0$$

is

$$(-\lambda)^{M+1} = 0 \qquad \text{(A.2)}$$

Since every linear transformation is annulled by its characteristic polynomial,[23] we have $(\mathbf{F}_M)^{M+1} = 0$.

Appendix B

We derive here, from the correlation functions in eq III.36, the prediction of the Hookean dumbbell model for

the material functions of a dilute solution. An expression for the stress tensor is derived in ref 2. In terms of the dimensionless coordinates used here, the polymer contribution to the stress tensor is

$$\tau_p = nkT[-\beta V_0\langle \vec{R}^*\vec{R}^*\rangle + \mathbf{I}] \tag{B.1}$$

where n is the number density of dumbbells. The first term is the stress due to the tension in the springs. The second term is the stress due to the tension in the springs when the system is in equilibrium; the stress tensor includes only the stress that arises in response to the flow. From eq III.36, we have

$$\tau_p = -nkT\begin{pmatrix} 2\xi^2 & \xi & 0 \\ \xi & 0 & 0 \\ 0 & 0 & 0 \end{pmatrix} \tag{B.2}$$

From the stress tensor, we can determine the viscosity, the first normal stress coefficient Ψ_1, and the second normal stress coefficient Ψ_2. (See ref 2 for definitions.) The Hookean dumbbell model predicts

$$\eta - \eta_s = nkT\tau/4$$
$$\Psi_1 = nkT \tag{B.3}$$
$$\Psi_2 = 0$$

Contrary to experimental results, the material functions are predicted to be independent of shear rate. This points to the inadequacy of the Hookean dumbbell model.

Appendix C

We outline here the evaluation of the sums $\Delta^\circ_{ij}(t)$, $\Delta_1(ij,t)$, and $\Delta_2(ij,t)$, which are defined in eq IV.5 and IV.6. Details can be found in ref 20. We need that[2,20]

$$B_{i\nu}^{-1} = j/(N+1); \qquad j < \nu \le N+1$$
$$B_{i\nu}^{-1} = -[1 - j/(N+1)]; \qquad \nu \le j < N+1 \tag{C.1}$$
$$B_{i\nu}^{-1} = 1; \qquad j = N+1$$

With this expression for $\mathbf{B}^{-1}$ and eq II.26 for $\mathbf{U}$ and using Gradshteyn and Ryzhik[24] (1.342.1) and (1.352.1), we find after some algebra

$$\sum_{\mu=1}^{N} B_{i\mu}U_{\mu\nu} = -\left(\frac{2}{N+1}\right)^{-1/2} \frac{1}{2\sin\left(\frac{\nu\pi}{2(N+1)}\right)} \cos\left(\frac{2i-1}{2}\,\frac{\nu\pi}{N+1}\right) \tag{C.2}$$

Using this result in eq IV.5, we find

$$\Delta^\circ_{ij}(t) = 3\left(\frac{2}{N+1}\right)\sum_\nu \frac{1}{a_\nu}\{[\cos((i+j-1)\theta)\cos((i-j)\theta) - 1] + [1 - \cos((i-j)\theta)\exp(-a_\nu t)] + [1 - \cos((i+j-1)\theta)\exp(-a_\nu t)]\} \tag{C.3}$$

where $\theta \equiv \nu\pi/(N+1)$ and we have added and subtracted $1/a_\nu$ from the summand and regrouped terms. For $N \gg 1$ and $t \ll N^2$, this sum can be replaced by an integral. (The restriction $t \ll N^2$ arises from taking the lower limit to be zero.) We find

$$\Delta^\circ_{ij}(t) = 3\{I_0(i-j) + I_0(i+j-1) + \frac{2}{\pi}\int_0^\infty \frac{d\theta}{\theta^2}[\cos((i+j-1)\theta)\cos((i-j)\theta) - 1] \tag{C.4}$$

where

$$I_0(s,t) = \frac{2}{\pi}\int_0^\infty \frac{d\theta}{\theta^2}[1 - \cos(\theta s)\exp(-\theta^2 t)] \tag{C.5}$$

These integrals can be evaluated by replacing θ^2 by $\theta^2 + \epsilon^2$, integrating term by term (using GR[24] (3.723.2) and (3.954.2)), and then taking $\epsilon \to 0$. The result is

$$\Delta^\circ_{ij}(t) = 3\{I_0(i-j,t) + I_0(i+j-1,t) - (i+j-1)\}$$

where

$$I_0(s,t) = |s|\Phi\left(\frac{s}{2t^{1/2}}\right) + 2\left(\frac{6}{\pi}\right)^{1/2}\exp(-s^2/4t) \tag{C.6}$$

and Φ is the probability integral.

$\Delta_1(ij,t)$ can be evaluated in a manner analogous to Δ°_{ij}, except that terms will appear that would diverge if the sum were approximated by an integral. These terms must be isolated and summed directly. Using eq C.2 in the definition in eq IV.6, we find

$$\Delta_1(ij,t) = \frac{2}{N+1}\sum_{\nu=1}^{N}\frac{1}{a_\nu^2}[1 + \cos((i+j-1)\theta)\cos((i-j)\theta)] - [\cos((i-j)\theta) + \cos((i+j-1)\theta)]\underline{(1 - a_\nu t)} - [\cos((i-j)\theta) + \cos((i+j-1)\theta)](\exp(-a_\nu t) \underline{- 1 + a_\nu t}) \tag{C.7}$$

We have added and subtracted the underlined terms. The first two terms diverge as $\theta \to 0$, and, therefore, they cannot be approximated by an integral. (This is a consequence of strong dependence on N.) However, they can be summed directly by using GR[24] (1.443.3) and (1.443.6), along with the product formula for cos A cos B. The last term can be approximated by an integral, which can then be evaluated in a manner analogous to that used for Δ°_{ij}.

When eq C.2 is substituted into $\Delta_2(ij,t)$ in eq IV.6, terms appear that diverge even more strongly as $\theta \to 0$ than those in $\Delta_1(ij,t)$, as a consequence of even stronger N dependence. As in Δ_1, these terms can be isolated and summed exactly. We find

$$\Delta_2(ij,t) = \left(\frac{2}{N+1}\right)\sum_{\nu=1}^{N}\left(\frac{1}{a_\nu^3}\right)[1 + \cos((i+j-1)\theta)\cos((i-j)\theta)] - \underline{[\cos((i-j)\theta) + \cos((i+j-1)\theta)](1 - a_\nu t + a_\nu^2 t^2)} - [\cos((i-j)\theta) + \cos((i+j-1)\theta)] \times [\exp(-a_\nu t) \underline{- 1 + a_\nu t - a_\nu^2 t^2}]$$

(where, again, we have added and subtracted the underlined terms.) The first two terms can be summed exactly, while the last term can be approximated by an integral, which can then be evaluated exactly. The full results for $\Delta_1(ij,t)$ and $\Delta_2(ij,t)$ can be found in ref 20. Some interesting limits are given and discussed in section IV.

References and Notes

(1) Yamakawa, H. *Modern Theory of Polymer Solutions*; Harper and Row: New York, 1971.
(2) Bird, R. B.; Hassager, O.; Armstrong, R. C.; Curtiss, C. F. *Dynamics of Polymeric Liquids: Kinetic Theory*; Wiley: New York, 1977; Vol. II.
(3) Williams, M. C. *AIChE J.* **1977**, *21*(1), 1.
(4) Bird, R. B. *J. Rheol.* **1982**, *26*(3), 277.
(5) Resibois, P.; DeLeener, M. *Classical Kinetic Theory of Fluids*; Wiley: New York, 1977. (The Fokker–Planck equation is derived for a single particle; the generalization to a many-particle system is straightforward.)
(6) Kramers, H. A. *Physics* **1940**, *7*(4), 284.
(7) Booij, H. C. *J. Chem. Phys.* **1984**, *80*(9), 4571. Stasiak, W.; Cohen, C. *J. Chem. Phys.* **1983**, *78*(1), 553.
(8) Recently, Honerkamp and Öttinger (Freiburg Preprint THEP 85/9) used field theoretic techniques to determine the dynam-

ical behavior of a nonlinear dumbbell model in steady shear flow. The time correlation functions that we derive in section III agree with their more general results. In addition, Jilge et al. (Jilge, W.; Hess, W.; Klein, R. *J. Polym. Sci., Polym. Phys. Ed.* **1983**, *23*, 1079) have studied the dynamic structure factor of linear dumbbells in shear flow.
(9) Dotson, P. J. *J. Chem. Phys.* **1983**, *79*(11), 5730.
(10) Stasiak, W.; Cohen, C. *J. Chem. Phys.* **1983**, *79*(11), 5718. Fuller, G. G. *J. Polym. Sci., Polym. Phys. Ed.* **1983**, *21*, 151. King, D. H.; James, D. F. *J. Chem. Phys.* **1983**, *78*(7), 4743. Lodge, A. S.; Wu, Y. *Rheol. Acta* **1971**, *10*, 539. van Wiechen, P. H.; Booij, H. C. *J. Eng. Math.* **1971**, *5*(2), 89. The last three papers exhibit general stationary-state solutions to the SE for a linear chain in an arbitrary flow field.
(11) Rouse, P. E. *J. Chem. Phys.* **1953**, *21*, 1272.
(12) Öttinger, H. C. *J. Chem. Phys.* **1986**, *84*(7), 4086. Öttinger, H. C. Preprint, Aug 1985. Honerkamp, J.; Öttinger, H. C. Preprint, Oct 1985. Biller, P.; Öttinger, H. C.; Petruccione, F. Preprint, Jan 1986. Öttinger, H. C. Preprint, Mar 1986.
(13) Fixman, M. *J. Chem. Phys.* **1966**, *45*(3), 793.
(14) Edwards, S. F.; Freed, K. F. *J. Chem. Phys.* **1974**, *61*(3), 1189.
(15) Stockmayer, W. H. In *Molecular Fluids*; Balian, R., Weill, G., Eds.; Gordon and Breach: New York, 1976.
(16) The Bose representation of a quantum harmonic oscillator can be found in many introductory quantum texts. See, for example: Merzbacher, E. *Quantum Mechanics*, 2nd ed.; Wiley: New York, 1961. Schiff, L. I. *Quantum Mechanics*, 3rd ed.; McGraw-Hill: New York, 1955.
(17) Guyer, R. A. *Phys. Rev. A* **1982**, *26*(2), 1062.
(18) Byron, F. W., Jr.; Fuller, R. W. *Mathematics of Classical and Quantum Physics*; Addison-Wesley: Reading, MA, 1969; Vol. I.
(19) Bird, R. B.; Saab, H. H.; Dotson, P. J.; Fan, X. J. *J. Chem. Phys.* **1983**, *79*(11), 5729.
(20) Johnson, J. A. Y. Ph.D. Thesis, University of Massachusetts, Amherst, MA, Feb 1985.
(21) de Gennes, P.-G. *Physics (Long Island City, N.Y.)* **1967**, *3*(1), 37.
(22) Brout, R.; Carruthers, P. *Lectures on the Many-Electron Problem*; Interscience: New York, 1963.
(23) Halmos, P. R. *Finite Dimensional Vector Spaces*, 2nd ed.; Van Nostrand: New York, 1958.
(24) Gradshteyn, I. S.; Ryzhik, I. M. *Table of Integrals, Series and Products* (corrected and enlarged edition); Academic: New York, 1980. Referred to as GR followed by the formula number.

Dynamics of an Entangled Chain in an External Field†

Douglas Adolf

Sandia National Laboratories, Albuquerque, New Mexico 87185. *Received June 17, 1986*

ABSTRACT: A straightforward model for the dynamics of an entangled macromolecule in an external field is presented. The model balances the frictional drag forces, random thermal forces, and the external body forces acting on a chain confined to a tube by entanglements with its neighbors. The calculated center-of-mass velocity is found to be in agreement with experiment and current theories, and the center-of-mass diffusion coefficients parallel and transverse to the external field are predicted to increase with increasing field strength. The time required for a chain to renew its configuration is predicted to decrease with increasing field strength. The results of a computer simulation based on this model are in agreement with theory.

Introduction

The self-diffusion of linear entangled polymers seems to be well described by the reptation theory of de Gennes.[1,2] Of present interest is the effect of an external body force on this mechanism of diffusion.[3-8] The most important example of this process is gel electrophoresis where DNA molecules of differing molecular weights that are forced through a gel by an applied electric field can be separated with extreme sensitivity. Of course, other body forces should have similar effects on the dynamic properties, and experiments to test this can be envisioned: gel sedimentation where a centrifugal force separates chains of different molecular weights and the self-diffusion of a tracer chain in a chemical potential gradient formed by the interdiffusion of two miscible polymers.

Several theories have been proposed to determine the dynamics of an entangled polymer in an external field. Those of Lumpkin and co-workers[3,4] and Slater and Noolandi[5,6] are based on modifications of the version of reptation set forth by Doi and Edwards.[9] In this model, an entangled chain is viewed as being trapped in a tube that prohibits motion perpendicular to its contour and, therefore, the chain is forced to follow the tube's contour by the set of equations

$$\mathbf{r}_n(t+\Delta t) = \{[1+\xi(t)]/2\}\mathbf{r}_{n+1}(t) + \{[1-\xi(t)]/2\}\mathbf{r}_{n-1}(t) \qquad (2 \le n \le N-1)$$

$$\mathbf{r}_1(t+\Delta t) = \{[1+\xi(t)]/2\}\mathbf{r}_2(t) + \{[1-\xi(t)]/2\}[\mathbf{r}_1(t)+\mathbf{v}(t)] \quad (1)$$

$$\mathbf{r}_N(t+\Delta t) = \{[1+\xi(t)]/2\}[\mathbf{r}_N(t)+\mathbf{v}(t)] + \{[1-\xi(t)]/2\}\mathbf{r}_{N-1}(t)$$

where $\mathbf{r}_i(t)$ is the position of the ith monomer at time t, $\mathbf{v}(t)$ is a random vector of segment length a, which defines the orientation of a terminal segment as it leaves the tube, and $\xi(t)$ is randomly 1 or −1, depending on which end of the chain leads. Lumpkin et al. calculated the center-of-mass velocity[4] and found agreement with experimental observations that the velocity is inversely proportional to the molecular weight for low molecular weights and is independent of it at higher values.[10-12] They were not, however, concerned with deriving a complete theory for the dynamics of entangled chains in an external field, as is the goal of the present study. Slater and Noolandi[5] do propose such a theory, and the differences between their theory and ours will be discussed later in this paper.

Olvera de la Cruz et al.[8] approached this problem in a completely different manner. They simulated an entangled macromolecule in an electric field by a chain moving via modified Verdier-Stockmayer dynamics[13,14] in the presence of a fixed obstacle net and an external field. The chain relaxation time in their simulation actually increased with increasing field strength. At first this result seems

†This work performed at Sandia National Laboratories supported by the U.S. Department of Energy under Contract No. DE-AC04-76DP00789.

0024-9297/87/2220-0116$01.50/0